

Weakly coupled one-dimensional Mott insulators

Fabian H. L. Essler¹ and Alexei M. Tsvelik²¹*Department of Physics, University of Warwick, Coventry CV4 7AL, United Kingdom*²*Department of Physics, Brookhaven National Laboratory, Upton, New York 11973-5000*

(Received 3 October 2001; published 8 March 2002)

We consider a model of one-dimensional Mott insulators coupled by a weak interchain tunneling t_{\perp} . We first determine the single-particle Green's function of a single chain by exact field-theoretical methods and then take the tunneling into account by means of a random-phase approximation. In order to embed this approximation into a well-defined expansion with a small parameter, the Fourier transform $T_{\perp}(k)$ of the interchain coupling is assumed to have a small support in momentum space such that every integration over transverse wave vector yields a small factor $\kappa_0^2 \ll 1$. When $T_{\perp}(0)$ exceeds a critical value, a small Fermi surface develops in the form of electron and hole pockets. We demonstrate that Luttinger's theorem holds both in the insulating and in the metallic phases. We find that the quasiparticle residue Z increases very fast through the transition and quickly reaches a value of about 0.4–0.6. The metallic state close to the transition retains many features of the one-dimensional system in the form of strong incoherent continua.

DOI: 10.1103/PhysRevB.65.115117

PACS number(s): 71.10.Pm, 72.80.Sk

I. INTRODUCTION

The problem of the Mott metal-insulator transition, which is a consequence of electron interactions and not due to the band structure, has been the subject of great interest¹ since the pioneering works by Mott.² In 1964, Hubbard suggested a solution of this problem for a particular model.³ The key point of Hubbard's approach was to take into account the on-site Coulomb interaction U in perturbation theory in t/U . Unfortunately, the transition from the metallic to the insulating phase is expected to occur when the tunneling matrix element t is comparable to the on-site repulsion U . In this regime expansions in either t/U or U/t are not applicable. To overcome this difficulty, various approaches have been suggested. One of them considers a $SU(N)$ -symmetric generalization of the electronic model and carries out a $1/N$ expansion.^{4,5} Another approach is based on the so-called dynamical mean-field theory, which considers a lattice in infinitely many dimensions $D \rightarrow \infty$ (see Ref. 6 and references therein and also Refs. 7,8).

In this paper we follow a different route. We consider a quasi-one-dimensional model of interacting electrons, where the tunneling along one direction is much larger than along all others. This model can be described in terms of weakly coupled chains. When the band is half-filled and the interchain tunneling is switched off, Umklapp processes dynamically generate a spectral gap M . The same mechanism can generate gaps at *any* commensurate filling, e.g., quarter-filling, but only if the interactions are sufficiently strong. In the half-filled case the decoupled chains develop a Mott-Hubbard gap for any positive value of $U > 0$. In what follows we shall assume that the interchain tunneling is weak but *long ranged*, such that the Fourier transform of the interchain tunneling matrix element has two strong peaks in the Brillouin zone, one around zero wave vector and the other one around $\mathbf{Q} = (0, \pi, \pi)$ such that

$$T_{\perp}(\mathbf{k}) = -T_{\perp}(\mathbf{k} + \mathbf{Q}). \quad (1)$$

Due to the long-range character of the tunneling, the width of these peaks, denoted by κ_0 , is small ($\kappa_0 \ll 1$). Hence, every integration over the transverse momentum yields a small parameter κ_0^2 . The main idea of our approach is to treat the individual chains nonperturbatively and then to employ the random-phase approximation (RPA) to take into account the interchain tunneling. Since the Mott metal-insulator transition is associated with development of a coherent single-particle excitation branch, the correlation function we are interested in is the single-electron Green's function G . The RPA expression for G is

$$G(\omega, q, \mathbf{k}) = [G_0^{-1}(\omega, q) - T_{\perp}(\mathbf{k})]^{-1}, \quad (2)$$

where q is the momentum along the chain direction and G_0 is the single-particle Green's function for an individual chain. The corrections to RPA are of higher order in κ_0^2 , which is the small parameter in our expansion. The smallness of κ_0^2 suppresses multiparticle tunneling processes, which generate exchange interactions between the chains and eventually lead to a three-dimensional phase transition. However, for small κ_0^2 the temperature at which this transition occurs is much smaller than the characteristic energy scale M of the problem. Therefore, throughout the paper we shall assume that we work at temperatures much smaller than M (such that the thermal effects on the single-particle Green's function can be neglected) but much larger than the transition temperature T_c , i.e., $T_c \ll T \ll M$. We note that an analogous RPA has been used by Wen⁹ to study weakly coupled Luttinger liquids (LL), see also Ref. 10 for a derivation based on functional integrals. An improved calculation for the case of coupled LL's has recently been carried out by Arrigoni.¹¹ It is based on taking into account multipoint correlation functions of uncoupled chains in a controlled way. In a Mott insulator multipoint correlation functions are much more difficult to determine than in a LL. We, therefore, postpone the discussion of corrections to RPA until future publications.

We also neglect the long-distance tails of the Coulomb interaction. This can be justified at finite temperatures if the dielectric constant at small frequencies is large.

The basic input of our approach is G_0 . To calculate this function we assume that for an isolated chain the Mott-Hubbard gap M is much smaller than the bandwidth D_{\parallel} . In this case one can use the continuous field-theoretical description in the low-energy limit. The corresponding field theory will be described in detail in the following section and is highly universal; all information about the underlying lattice model is incorporated in just three dimensionless constants. Thus, our assumptions can be summarized by the inequalities

$$D_{\parallel} \gg M \approx t_{\perp}(0) \gg t_{\perp}(|k| > \kappa_0),$$

$$T_c \ll T \ll M, \quad (3)$$

where the Mott-Hubbard gap M is a function of the interactions. The smallness of M does not imply that the interactions are weak. For example, in the one-dimensional (1D) Hubbard model the field-theoretical description works well even for U/t as large as 2–3 (see, for example, Ref. 12). At such interaction strength one should expect the spin and charge velocities to be considerably different. This is a consequence of spin-charge separation, which is one of the most interesting features of one-dimensional strongly correlated systems. The effects of spin-charge separation in the insulating regime deserve a special discussion, which will be given later in the paper.

The outline of this paper is as follows. In Sec. II we introduce the model and in Sec. III we discuss the limit of decoupled chains. In Sec. IV we take the interchain coupling into account within RPA. In Sec. V we discuss the formation of a Fermi surface. In Sec. VI we determine various physics properties and in Sec. VII we discuss possible applications to quasi-1D organic conductors.

II. THE MODEL

We take as a starting point the following lattice model of correlated electrons

$$H = \sum_l H^{(l)} + \sum_{l,m,n,\sigma} t_{lm} c_{n,\sigma}^{(l)\dagger} c_{n,\sigma}^{(m)} + \text{H.c.},$$

$$H^{(l)} = -t \sum_{n,\sigma} c_{n,\sigma}^{(l)\dagger} c_{n+1,\sigma}^{(l)} + \text{H.c.} + U \sum_n n_{j,\uparrow}^{(l)} n_{j,\downarrow}^{(l)}. \quad (4)$$

Here l, m label Hubbard chains and n labels the sites along a given chain. In the physically most interesting situation the interchain hopping matrix elements t_{lm} are taken to be equal to t_{\perp} if l and m are nearest neighbors and zero otherwise. For this choice of interchain hopping our calculational scheme is uncontrolled: there is no small expansion parameter. One may nevertheless, apply our scheme and hope that the corrections are small in some regime of temperatures. On the other hand, one may choose the t_{nm} 's in such a way that a small expansion parameter is introduced, as explained above and in more detail in Appendix A.

Let us first consider the case of uncoupled chains $t_{\perp} = 0$. For weak repulsion $U < t$ and low energies, a field-theory description is appropriate. Keeping only modes in the vicinity of the Fermi momenta $\pm k_F = \pm \pi/2a_0$, we may decompose the lattice Fermi operators as

$$c_{n,\sigma}^{(l)} = \sqrt{a_0} [\exp(ik_F x) R_{\sigma}^{(l)}(x) + \exp(-ik_F x) L_{\sigma}^{(l)}(x)], \quad (5)$$

where a_0 is the lattice spacing. Inserting this prescription into the Hamiltonian (4) and dropping the chain index (l) for the time being, one obtains

$$\mathcal{H} = \sum_{\sigma} v_F \int dx [L_{\sigma}^{\dagger} i \partial_x L_{\sigma} - R_{\sigma}^{\dagger} i \partial_x R_{\sigma}] + \frac{g}{3} \int dx [\mathbf{I} \cdot \mathbf{I} + : \bar{\mathbf{I}} \cdot \bar{\mathbf{I}} : - : \mathbf{J} \cdot \mathbf{J} : - : \bar{\mathbf{J}} \cdot \bar{\mathbf{J}} :] + 2g \int dx [\mathbf{I} \cdot \bar{\mathbf{I}} - \mathbf{J} \cdot \bar{\mathbf{J}}], \quad (6)$$

where $v_F = 2ta_0$ is the Fermi velocity and $g = Ua_0$. Here \mathbf{J} and \mathbf{I} are the chiral components of SU(2) spin and pseudospin currents

$$I^3 = \frac{1}{2} \sum_{\sigma} : L_{\sigma}^{\dagger} L_{\sigma} :, \quad I^{\pm} = L_{\uparrow}^{\dagger} L_{\downarrow}^{\dagger},$$

$$\bar{I}^3 = \frac{1}{2} \sum_{\sigma} : R_{\sigma}^{\dagger} R_{\sigma} :, \quad \bar{I}^{\pm} = R_{\uparrow}^{\dagger} R_{\downarrow}^{\dagger},$$

$$J^3 = \frac{1}{2} (L_{\uparrow}^{\dagger} L_{\uparrow} - L_{\downarrow}^{\dagger} L_{\downarrow}), \quad J^{\pm} = L_{\uparrow}^{\dagger} L_{\downarrow},$$

$$\bar{J}^3 = \frac{1}{2} (R_{\uparrow}^{\dagger} R_{\uparrow} - R_{\downarrow}^{\dagger} R_{\downarrow}), \quad \bar{J}^{\pm} = R_{\uparrow}^{\dagger} R_{\downarrow}. \quad (7)$$

By employing the Sugawara construction, the Hamiltonian (6) can now be split into two parts, corresponding to the spin and charge sectors, respectively¹³

$$\mathcal{H} = \mathcal{H}_c + \mathcal{H}_s,$$

$$\mathcal{H}_s = \frac{2\pi v_s}{3} \int dx [: \mathbf{J} \cdot \mathbf{J} : + : \bar{\mathbf{J}} \cdot \bar{\mathbf{J}} :] - 2g \int dx \mathbf{J} \cdot \bar{\mathbf{J}},$$

$$\mathcal{H}_c = \frac{2\pi v_c}{3} \int dx [: \mathbf{I} \cdot \mathbf{I} : + : \bar{\mathbf{I}} \cdot \bar{\mathbf{I}} :] + 2g \int dx \mathbf{I} \cdot \bar{\mathbf{I}}. \quad (8)$$

Here $v_s = v_F - Ua_0/2\pi$ and $v_c = v_F + Ua_0/2\pi$. Apart from the (marginally) irrelevant current-current interaction in the spin sector and the difference in spin and charge velocities, the Hamiltonian (8) is identical to the one of the SU(2) Thirring model. The latter can be bosonized in terms of a Sine-Gordon model and a free boson; the resulting Lagrangian density is

$$\mathcal{L}_s = \frac{1}{16\pi} [v_s^{-1} (\partial_{\tau} \Phi_s)^2 + v_s (\partial_x \Phi_s)^2],$$

$$\mathcal{L}_c = \frac{1}{16\pi} [v_c^{-1} (\partial_{\tau} \Phi_c)^2 + v_c (\partial_x \Phi_c)^2] + \lambda \cos(\beta \Phi_c), \quad (9)$$

where $\beta=1$. If we consider additional small density-density interactions between nearest-neighbor sites in Eq. (4) the field-theory limit is again of the form (9), but now $\beta<1$. Using the integrability of the model (9) it is possible to determine dynamical correlation functions. This is the subject of the following section.

III. UNCOUPLED CHAINS

The calculation of the spectral function for half-filled Mott insulators is based on the following principles.

a. Locality. R_α and L_α are local fields. This allows us to employ the standard form-factor approach.¹⁴ Some important elements of this approach are summarized in Appendix B.

b. Spin-charge separation. The Hamiltonian (8) is the sum of two parts representing the spin and charge degrees of freedom, respectively. By means of bosonization one can represent R_α and L_α as products of operators belonging to the two different sectors. For example,

$$R_\sigma^\dagger = \frac{\eta_\sigma}{\sqrt{2\pi}} \exp\left(\frac{i}{2}\phi_c\right) \exp\left(\pm\frac{i}{2}\phi_s\right), \quad (10)$$

where ϕ_c and ϕ_s are chiral components of the bosonic fields, η_σ are Klein factors and the plus (minus) sign corresponds to $\sigma=\uparrow$ ($\sigma=\downarrow$). The operators on the right-hand side of Eq. (10) are nonlocal with respect to the canonical Bose fields $\Phi_{c,s}$. Nevertheless, Eq. (10) implies that form factors of R_σ also factorize into charge and spin parts, at least in the limit when one of the sectors becomes massless.

c. "Triviality" of the spin sector. In the limit $g_s\rightarrow 0$ the field theory for the spin sector becomes massless and the correlation function of the spin exponent in Eq. (10) is simply given by

$$\left\langle \exp\left[\frac{i}{2}\phi_s(x,\tau)\right] \exp\left[-\frac{i}{2}\phi_s(0)\right] \right\rangle = \frac{1}{\sqrt{v_s\tau - ix}}. \quad (11)$$

d. Lorentz invariance and Watson's theorem. Let us consider form factors of the left moving Fermi operator $L_\sigma(x)$. The first nonvanishing form factor is between the vacuum and a scattering state of one spinon (with spin σ) and one antiholon. We denote the rapidity of the spinon (antiholon) by θ_s (θ_c) (our notations are summarized in Appendix B). Lorentz invariance and Watson's theorem impose the following form for the first nonvanishing form factor for the fermion operator

$$\langle 0|L_\sigma(0)|\theta_c, \theta_s\rangle_{\bar{h}s} = \exp[(\theta_c + \theta_s)/4]f(\theta_c - \theta_s). \quad (12)$$

The function $f(\theta)$ is periodic with period $2i\pi$ and does not contain poles. Furthermore, the usual asymptotic bound¹⁶ yields

$$\lim_{\theta_\alpha\rightarrow\infty} \langle 0|L|\theta_c, \theta_s\rangle \exp\left(-\frac{\theta_\alpha}{4}\right) \leq \text{const}, \quad (13)$$

where $\alpha=c,s$. This leaves us with the only possibility $f(\theta) = \text{const}$. As we see, this matrix element does not depend on the anisotropy of the interaction (apart from the constant

prefactor f). The reason for this is that all information about the anisotropy of the coupling constants is contained in the two-particle S matrices of holons and spinons and does not influence the single-particle emission. The matrix element (12) describes the emission of one kink in the charge and one kink in the spin sector. The charge part of this first term in the expansion is thus, equal (up to an overall numerical factor) to

$$\begin{aligned} & \int_{-\infty}^{\infty} d\theta e^{\theta/2} \exp\left[-m\tau \cosh\theta - im\frac{x}{v_c} \sinh\theta\right] \\ &= \left(\frac{\tau v_c - ix}{\tau v_c + ix}\right)^{1/4} K_{1/2}(m\sqrt{\tau^2 + x^2 v_c^{-2}}) \\ &\propto \frac{\exp[-m\sqrt{\tau^2 + x^2 v_c^{-2}}]}{\sqrt{v_c\tau + ix}}. \end{aligned} \quad (14)$$

In the next step we use the fact that the single-electron Green's function factorizes into a charge and a spin piece. Let us consider intermediate states containing a single antiholon and any number of spinons. Factorization implies that if we carry out the sum over all multispinon contributions, we must obtain the conformal result (11) for the spin sector. Therefore, we arrive at the following result for the two-point function

$$\langle L_\sigma(x,\tau)L_\sigma^\dagger(0,0)\rangle \simeq \frac{Z_0}{2\pi} \frac{\exp[-m\sqrt{\tau^2 + x^2 v_c^{-2}}]}{\sqrt{(v_s\tau + ix)(v_c\tau + ix)}}, \quad (15)$$

where¹⁵

$$Z_0 \approx 0.9218. \quad (16)$$

The leading corrections to Eq. (16) involve intermediate states containing two antiholons and one holon and are thus of order $O[\exp(-3m\tau)]$. Similarly we have

$$\langle R_\sigma(x,\tau)R_\sigma^\dagger(0,0)\rangle \simeq \frac{Z_0}{2\pi} \frac{\exp[-m\sqrt{\tau^2 + x^2 v_c^{-2}}]}{\sqrt{(v_s\tau - ix)(v_c\tau - ix)}}. \quad (17)$$

Equations (16) and (17) were first written down by Wiegmann (for $v_c=v_s$).¹⁷ This remarkable result appears to have been subsequently forgotten and rediscovered only much later by Voit, who conjectured the same form for the Green's function.¹⁸ The correct form was again reproduced by Starykh *et al.*,¹⁹ although on the basis of arguments that cannot be accepted as rigorous. An earlier attempt to calculate the single-particle Green's function using the form-factor approach²⁰ led to an incorrect result yielding a K_1 modified Bessel function instead of $K_{1/2}$ in Eq. (15). Finally, Parola and Sorella²¹ determined the spectral function by mapping the problem of a single hole in a Mott insulator onto an effective spin chain with skew boundary conditions. Their results are somewhat implicit so that it is difficult to compare them to Eq. (17).

To conclude this section we would like to remark that the above results can be generalized to the case of the $SU(N)$ Thirring model

$$\begin{aligned} \langle L_\sigma(x, \tau) L_\sigma^\dagger(0, 0) \rangle &= \frac{Z_0(N)}{2\pi} \frac{1}{(v_s \tau + ix)^{1/N}} \\ &\times \left(\frac{v_c \tau - ix}{v_c \tau + ix} \right)^{[(1/2) - (1/2N)]} \\ &\times K_{1-(1/N)}(m \sqrt{\tau^2 + x^2 v_c^{-2}}). \end{aligned} \quad (18)$$

Here we have used that the kinks in the $SU(N)$ Thirring model have spin $\frac{1}{2}(1 - [1/N])$.²² A similar formula with $x \rightarrow -x$ holds for the right-moving fermions.

A. Short-distance behavior: Renormalization-group calculations

Strictly speaking, single-kink emissions in the charge sector allows one to consider only frequencies less than $3m$, which is the threshold for the emission of two antiholons and one holon. However, since the numerical value of Z_0 is quite close to 1 Eqs. (16) and (17) are likely to provide a very good description of the Green's function in the entire frequency interval. Indeed, considering the short-distance (high-energy) behavior ($m \sqrt{\tau^2 + x^2 v_c^{-2}} \ll 1$) in Eqs. (17) and (16) we recover the standard expressions for the Green's functions of the Luttinger liquid (modulo the prefactor Z_0 , which, as we have said, is almost 1). A better description of the short-distance behavior is obtained by carrying out a renormalization-group (RG) analysis. The RG equations for the coupling constant g and wave-function renormalization Z in the case $v_c = v_s = v$ are

$$g_0 = g + \frac{g^2}{2\pi} \ln \frac{\Lambda^2}{\mu^2} + \mathcal{O}(g^3), \quad (19)$$

$$Z = 1 - \frac{3}{32\pi^2} g^2 \ln \frac{\Lambda^2}{\mu^2} + \mathcal{O}(g^3), \quad (20)$$

where Λ is a UV cutoff and μ a subtraction point. The RG improved result for the two-point function is thus

$$\langle R_\sigma(x, \tau) R_\sigma^\dagger(0, 0) \rangle = \frac{Z(r)}{2\pi(v\tau - ix)}, \quad (21)$$

where

$$\begin{aligned} Z(r) &\approx 1 - \frac{3}{16\pi} g(r), \\ g(r) &\approx -\frac{\pi}{\ln(rm)}, \quad r^2 = x^2 + v^2 \tau^2 \ll m^{-2}. \end{aligned} \quad (22)$$

Comparing this to Eq. (17) for short distances, we find very good agreement. In the anisotropic case, where the short-distance behavior of the Green's function is controlled by the Luttinger liquid exponent, the agreement becomes worse. For "large" anisotropy it may become necessary to take intermediate states with, e.g., two solitons and one antisoliton into account in order to get a good description of the Green's function over a large range of energies.

B. Retarded dynamical Green's function

Given the expression (17) for the Green's function in position space we can calculate the dynamical Green's function by Fourier transformation and subsequent analytic continuation to real frequencies. A straightforward calculation gives the following result for the retarded Green's function

$$\begin{aligned} G_{RR}^{(R)}(\omega, k_F + q) &= -Z_0 \sqrt{\frac{2}{1 + \alpha}} \frac{\omega + v_c q}{\sqrt{m^2 + v_c^2 q^2 - \omega^2}} \\ &\times \left[(m + \sqrt{m^2 + v_c^2 q^2 - \omega^2})^2 \right. \\ &\left. - \frac{1 - \alpha}{1 + \alpha} (\omega + v_c q)^2 \right]^{-1/2}, \end{aligned} \quad (23)$$

where $\alpha = v_s/v_c$. At $\alpha = 1$ this simplifies to

$$G_{RR}^{(R)}(\omega, k_F + q) = -\frac{Z_0}{\omega - vq} \left[\frac{m}{\sqrt{m^2 + v^2 q^2 - \omega^2}} - 1 \right]. \quad (24)$$

C. Spectral function

The spectral function is defined as

$$A_{RR}(\omega, k_F + q) = -\frac{1}{\pi} \text{Im} G_{RR}^{(R)}(\omega, k_F + q). \quad (25)$$

In the limit $v_c = v_s = v$ we obtain from Eq. (24) the following simple result

$$A_{RR}(\omega, k_F + q) = \frac{Z_0 m}{\pi |\omega - vq|} \frac{\Theta(|\omega| - \sqrt{m^2 + v^2 q^2})}{\sqrt{\omega^2 - m^2 - v^2 q^2}}. \quad (26)$$

An explicit expression for the general case $v_s \neq v_c$ is easily obtained from Eq. (23). We note that the result is *exact* for energies $\omega \leq 3m$ as the intermediate states involving more than one antiholon will start contributing only at this energy. However, from previous experience²³ as well as on the basis of the arguments given above, we expect Eq. (23) to be an excellent approximation up to very high energies.

For general v_c, v_s the spectral function is nonvanishing in a region with boundary $\omega = \epsilon(p)$ defined by the equation

$$\epsilon(p) = \min_q [v_s |p - q| + \sqrt{v_c^2 q^2 + m^2}]. \quad (27)$$

The solution of this equation is

$$\epsilon(p) = \begin{cases} \sqrt{m^2 + v_c^2 p^2} \equiv \epsilon_0(p) & \text{if } p \leq Q \\ v_s p + m \sqrt{1 - \alpha^2} \equiv \epsilon_1(p) & \text{if } p \geq Q, \end{cases} \quad (28)$$

where

$$Q = \frac{m\alpha}{\sqrt{v_c^2 - v_s^2}}. \quad (29)$$

The spectral function generally has several kinds of singularities. First, there are singularities just above the threshold. For small momenta $|q| \ll Q$ there is a square-root singularity above the threshold $\omega = \epsilon(q)$

$$A(\omega, k_F + q) \approx \frac{Z_0}{\pi} \frac{\epsilon_0(q) + v_c q}{\sqrt{2\epsilon_0(q)}} [v_c q + \epsilon_0(q)]^{-1/2} \\ \times [\alpha \epsilon_0(q) - v_c q]^{-1/2} \frac{1}{\sqrt{\omega - \epsilon_0(q)}}. \quad (30)$$

There is also a square-root singularity above the threshold for “large” momenta $|q| \gg Q$, where

$$A(\omega, k_F + q) \approx \frac{Z_0}{\pi} \frac{1}{\sqrt{v_c - v_s}} \frac{1}{\sqrt{|q| - Q}} \frac{1}{\sqrt{\omega - \epsilon_1(q)}}. \quad (31)$$

This square-root singularity is a general feature of the half-filled Mott insulator and apparently holds for any ratio of the gap to the bandwidth. Calculations done for a model where this ratio is infinite²⁴ give the same singularity.

For $|q| \gg Q$ there is a second square-root singularity for $\omega \rightarrow \epsilon_0(q)$ from below

$$A(\omega, k_F + q) \approx \frac{Z_0}{\pi} \frac{\epsilon_0(q) + v_c q}{\sqrt{2\epsilon_0(q)}} [v_c q + \epsilon_0(q)]^{-1/2} \\ \times [v_c q - \alpha \epsilon_0(q)]^{-1/2} \frac{1}{\sqrt{\epsilon_0(q) - \omega}}. \quad (32)$$

For $q = Q$ these two singularities collapse onto a single one and we have

$$A(\omega, k_F + Q) \approx \frac{Z_0}{\pi} \left(\frac{1 + \alpha}{1 - \alpha} \right)^{1/4} 2^{-5/4} \epsilon(Q)^{-1/4} [\omega - \epsilon(Q)]^{-3/4}. \quad (33)$$

In Fig. 1 we show the spectral function for $v_c = v_s = v$ as a function of ω and q . As $Q = \infty$ in this case the threshold is simply given by $\omega = \sqrt{m^2 + v^2 q^2}$. The square-root singularities above the threshold are visible as regions of high spectral weight. Figure 2 shows a constant energy scan at $\omega = 3m$.

When we allow the spin and charge velocities to be different an interesting effect occurs as can be seen from the density plot of $A_{RR}(\omega, q)$ in Fig. 3. For momenta $q < Q$ the threshold occurs at the gap for a single soliton moving with momentum q and the spectral function looks very much similar to it as it did in the case $\alpha = 1$. However, at momenta $q > Q$ the threshold gets shifted to $\omega = v_s q + m \sqrt{1 - \alpha^2}$ and a lot of spectral weight is concentrated between this threshold and the line $\omega = \sqrt{m^2 + v_c^2 q^2}$, where a second singularity occurs (see above). This is shown in the constant energy scan Fig. 4. For large momenta $v_{s,c} q \gg m$ the double singularity at $\omega \approx v_{s,c} q$ is similar to what occurs in a Luttinger liquid.²⁵

The states located in the “wedge” $\epsilon_1(q) < \omega < \epsilon_0(q)$ correspond to a situation where the single antiholon carries only a small part of the total momentum and the remainder is made up by exciting (many) spinons. This effect is reminis-

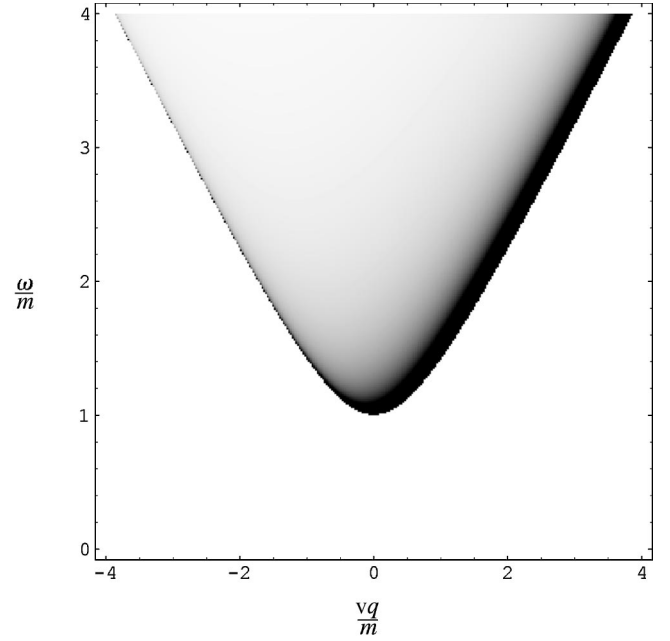


FIG. 1. Density plot of the spectral function $A_{RR}(\omega, k_F + q)$ as a function of ω/m and vq/m for $v_s = v_c = v$.

cent of Cherenkov radiation produced by a heavy particle moving through a medium with a speed greater than the speed of light in this medium. We note that this effect, as well as the smallness of the spectral weight in the region $q < 0$, is consistent with numerical studies of the Hubbard model at half-filling.²⁶

D. Tunneling density of states

From the Matsubara Green’s function at coinciding space points in model (8) we extract the single-particle density of states

$$\rho(\omega) = -2 \text{Im} G^{(R)}(\omega, x=0) = \frac{2Z_0}{\sqrt{v_s v_c}} \theta(|\omega| - m). \quad (34)$$

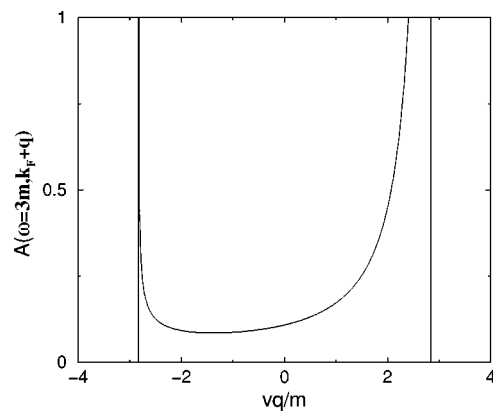


FIG. 2. Constant energy ($\omega = 3m$) scan of the spectral function for $\alpha = 1$.

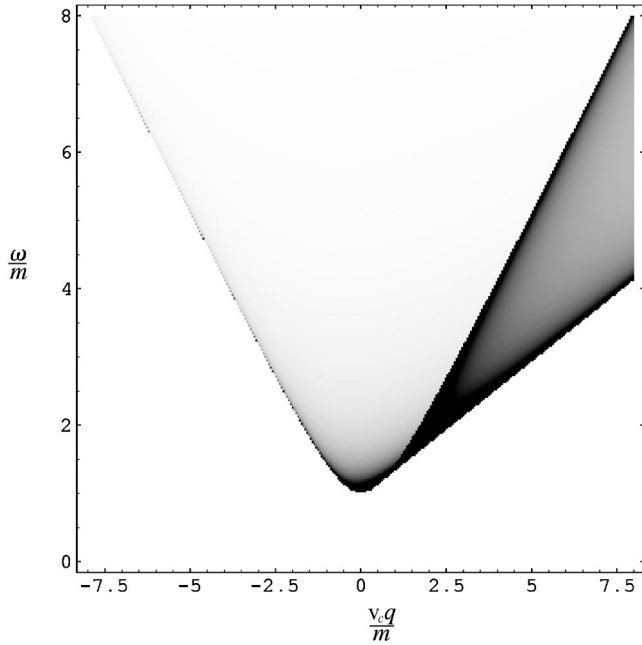


FIG. 3. Density plot of the spectral function $A_{RR}(\omega, k_F + q)$ as a function of ω/m and $v_c q/m$ for $\alpha=0.4$.

The density of states (34) is *constant* for energies higher than the single-particle gap m . Formula (34) is exact for $|\omega| \leq 3m$ and expected to be an excellent approximation up to very high (compared to the gap m) energies.

E. Momentum distribution function

From the time-independent Green's function we can calculate the momentum distribution function

$$n_\sigma(k_F + q) = \frac{1}{2} - \frac{Z_0}{\pi} \arctan\left(\frac{v_c q}{m}\right). \quad (35)$$

The momentum distribution function in the half-filled Hubbard model has recently been studied numerically using Density Matrix Renormalization Group (DMRG) in Ref. 27. For small values of U the numerical results are in agreement with Eq. (35).

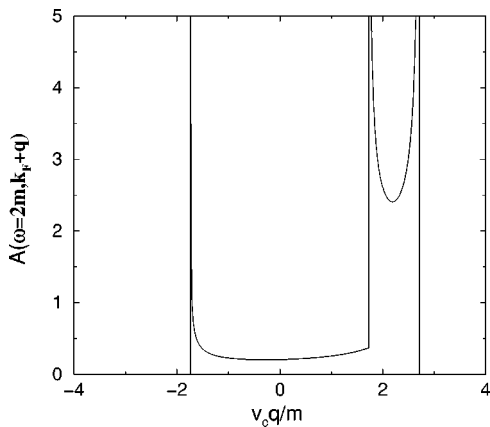


FIG. 4. Constant energy ($\omega=2m$) scan of the spectral function for $\alpha=0.4$.

IV. COHERENT SINGLE-PARTICLE MODE GENERATED BY THE INTERCHAIN TUNNELING

Taking the interchain tunneling into account in the RPA leads to an expression for the single-electron function of the form (2). The interchain tunneling gives rise to a branch of coherent excitations below the threshold of the 1D spectral function $A(\omega, q)$ in the region where $T_\perp(\vec{k}) < 0$. Therefore, even an *infinitesimal* interchain coupling leads to the coherent particle motion in the transverse direction and there is no confinement in the sense of Anderson.²⁸

A. $v_s = v_c$

Let us first discuss the case $v_s = v_c = v$. For very small interchain tunneling $|T_\perp(\vec{k})| \ll m$ the pole of Eq. (2) appears at a finite frequency very close to $\epsilon_0(p) = \sqrt{p^2 + m^2}$. In the vicinity of the pole we have

$$G(\omega, q, \vec{k}) \approx \frac{Z(q, \vec{k})}{\omega - \epsilon(q, \vec{k})}, \quad (36)$$

where $Z(q, \vec{k})$ varies strongly at small q and where for $|vq| \ll |m^2/Z_0 T_\perp(\vec{k})|$,

$$\epsilon(q, \vec{k}) = \epsilon_0(q) - \left(\frac{Z_0 T_\perp(\vec{k}) m}{\sqrt{2\epsilon_0(q)} [\epsilon_0(q) - vq]} \right)^2. \quad (37)$$

Along the chain direction, the dispersion of the coherent mode is asymmetric around $q=0$ and has a minimum at $vq \approx [Z_0 T_\perp(\vec{k})]^2/m$. For larger values of $T_\perp(\vec{k})$ this picture remains qualitatively unchanged although the dispersion law becomes more complicated. In the vicinity of the minimum the dispersion is approximately given by

$$\epsilon(q, \vec{k}) \approx \sqrt{\omega_0^2 + v^2(q - q_0)^2}, \quad (38)$$

where ω_0, q_0 depend only on $T_\perp(\vec{k})$. At large positive $vq \gg m$, we have

$$\epsilon(q, \vec{k}) \approx vq + Z_0 T_\perp(\vec{k}), \quad (39)$$

and at large negative $vq \ll -\max(m, |Z_0 T_\perp(\vec{k})|)$,

$$\epsilon(q, \vec{k}) \approx \sqrt{m^2 + (vq)^2} - \left[\frac{Z_0 T_\perp(\vec{k})}{2vq} \right]^2. \quad (40)$$

The dispersion of the coherent mode depends on the transverse momentum only through $T_\perp(\vec{k})$. In Fig. 5 we plot

$$E_x(q) \equiv \epsilon(q, \vec{k})|_{-Z_0 T_\perp(\vec{k}) = mx}, \quad (41)$$

as a function of q for several values of x . In Fig. 6 we plot the residue of the coherent mode for various x versus qv/m .

We see that $Z(q, \vec{k})$ is very small within the noninteracting Fermi surface.

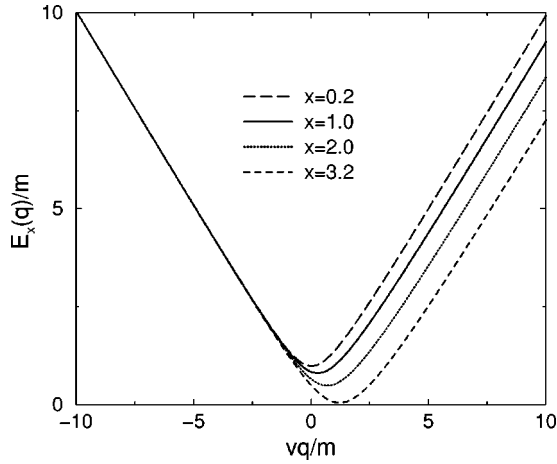


FIG. 5. Dispersion of the coherent mode along the chain direction for several values of $mx = -Z_0 T_\perp(\vec{k})$ and $\alpha = 1$.

B. $v_s \neq v_c$

The case of different velocities can be dealt with in a completely analogous way. In Fig. 7 we show the spectral function as a function of energy and momentum transfer along the chain direction for weak tunneling $-Z_0 T_\perp(\vec{k}) = m$. The coherent mode is clearly visible below the threshold of the one-dimensional spectral function.

In Fig. 8 we show a constant energy scan of the spectral function. If we compare Fig. 8 to the corresponding plot of the spectral function of uncoupled chains in Fig. 4, we notice that now there are two δ -function peaks corresponding to the coherent mode, and that the singularities of the incoherent scattering continuum have been smoothed out. It turns out that most ($\approx 75\%$) of the spectral weight for fixed $T_\perp(\mathbf{k})$ (i.e., we integrate only over q) is located in the coherent mode at q_2 , about 23% sits in the incoherent spinon-antiholon continuum and only 2% is due to the coherent branch at q_1 . The sharp difference between the weights in the coherent modes is consistent with the picture presented in Fig. 6.

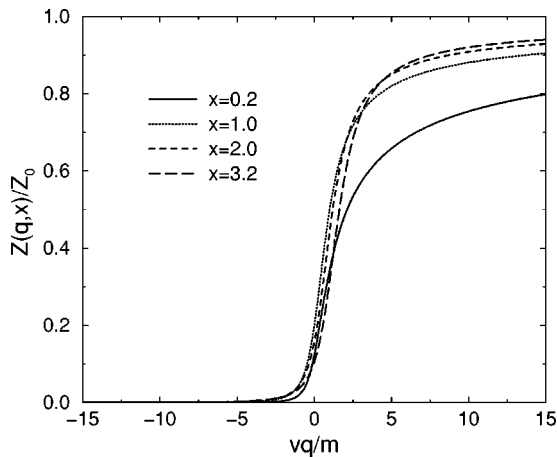


FIG. 6. Residue of the coherent mode as a function of the momentum along the chain direction for several values of $mx = -Z_0 T_\perp(\vec{k})$ and $\alpha = 1$.

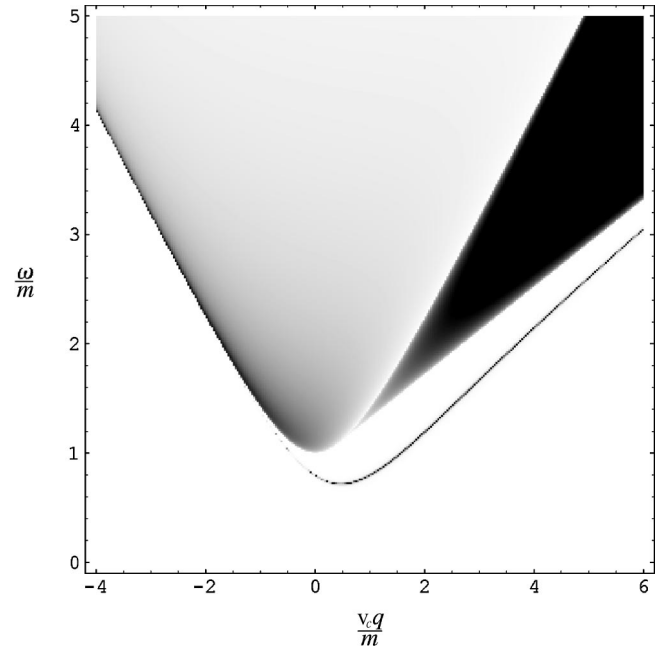


FIG. 7. Density plot of the spectral function $A_{RR}(\omega, q, \vec{k})$ as a function of ω and momentum transfer along the chain direction q for $\alpha = 0.4$ and $-Z_0 T_\perp(\vec{k}) = m$.

As t_\perp increases more and more of the spectral weight gets transferred to the coherent mode. For example, for $-Z_0 T_\perp(\vec{k}) = 3.2m$ approximately 95% of the spectral weight at energy $\omega = 2m$ is located in the coherent mode at q_2 . However, it is important to note that the coherent modes dominate only a small portion of the Brillouin zone [the part where $T_\perp(\mathbf{k})$ is large]. If we consider the total spectral weight, i.e., integrate over the transverse momentum \mathbf{k} as well, we find that the contribution of the coherent mode is generally small.

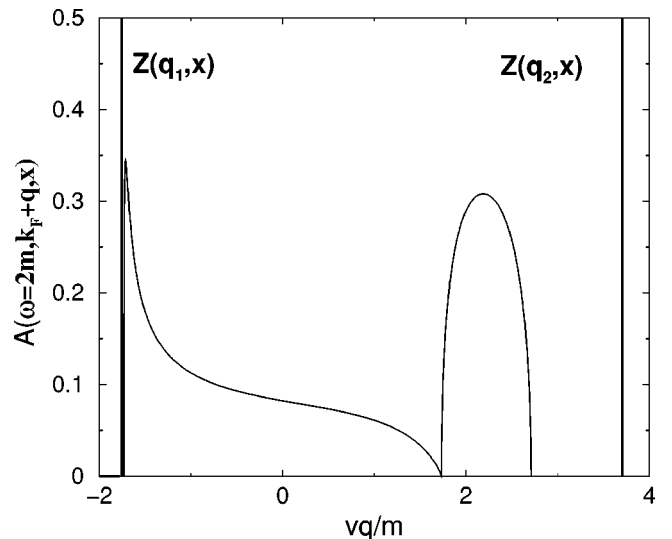


FIG. 8. $A_{RR}(\omega, q, \vec{k})$ as a function of the momentum along the chain direction for $\omega = 2m$, $\alpha = 0.4$, and $-Z_0 T_\perp(\vec{k}) = m$.

V. FERMI SURFACE AND LUTTINGER'S THEOREM

According to Luttinger's theorem the total number of particles in the system is proportional to the volume of momentum space included in the surface defined by the singularities of $\ln G(\omega=0, \mathbf{p})$. These singularities may be due to either poles or zeros of the single-particle Green's function. As was recently emphasized by Dzyaloshinskii,²⁹ the latter possibility must occur in Mott insulators thus removing an apparent violation of Luttinger's theorem. The Green's function (23) exhibits precisely this property: for $\omega=0$ it vanishes at $q=0$, which corresponds to the Fermi surface of the noninteracting system. Since the position of the zeros is unchanged in RPA, our results are in agreement with Luttinger's theorem.

When t_\perp exceeds a critical value, electronlike and holelike pockets of Fermi surface appear. The Fermi surface is determined by the equation

$$G_0^{-1}(0, q) = T_\perp(\mathbf{k}). \quad (42)$$

The volumes of electron and hole pockets are equal since $T_\perp(\mathbf{k}) = -T_\perp(\mathbf{Q} + \mathbf{k})$ where $\mathbf{Q} = (\pi, \pi, 0)$. So Luttinger's theorem continues to hold.

Using the fact that at $\omega=0$ the Green's function is always real, we get from Eq. (23)

$$\begin{aligned} [Z_0 T_\perp(\mathbf{k})]^2 &= \frac{(v_c^2 q^2 + m^2)(m + \alpha \sqrt{v_c^2 q^2 + m^2})}{\sqrt{v_c^2 q^2 + m^2} - m}, \\ \text{sgn}(T_\perp(\mathbf{k})) &= -\text{sgn}(q). \end{aligned} \quad (43)$$

The critical value of $T_\perp(\mathbf{k})$ necessary to produce the solution is

$$\left[\frac{Z_0 t_\perp^{\min}}{m} \right]^2 = 3 + \frac{9\alpha + 1}{2} x_0, \quad (44)$$

where x_0 is determined by the momentum q_0 where the Fermi surface first appears

$$x_0 = \sqrt{1 + v_c^2 q_0^2 / m^2} = \frac{3\alpha - 1 + \sqrt{1 + 10\alpha + 9\alpha^2}}{4\alpha}. \quad (45)$$

The critical value of $Z_0 t_\perp^{\min}$ varies from $2m$ at small v_s to $\sim 3.3m$ for $v_s = v_c$.

The residue at the Fermi surface is given by

$$Z = \frac{2Z_0}{(1+\alpha)} \frac{(x-1)}{x} \left[\frac{(x\alpha+1)}{(x+1)} \right]^{1/2}, \quad (46)$$

where $x \equiv \sqrt{1 + v_c^2 q^2 / m^2}$. Near the critical value of $T_\perp(\mathbf{k})$ the residue is numerically small but never goes to zero. For example, in the limit $v_s \rightarrow 0$ when $x=2$ we get

$$Z(v_s \rightarrow 0) \approx 0.58Z_0,$$

and at $v_s = v_c$ when $x \approx 1.62$ we have

$$Z(v_s = v_c) \approx 0.38Z_0.$$

For a cubic lattice with nearest-neighbor hopping the Fermi surface forms an *electron pocket* around $\tilde{q} = q_0 > 0$ and k_0^y

$= k_0^z = 0$ and *hole pockets* around $\tilde{q} = -q_0$ and $k_0^y = \pm \pi$, $k_0^z = \pm \pi$. The volume of the electron pocket is the same as the sum of the volumes of the hole pockets. When the pockets are very small their shape can be determined by expanding Eq. (43) around the point $(\mathbf{0}, q_0)$, using that

$$T_\perp(\mathbf{k}) \approx T_\perp(\mathbf{0}) [1 - \mathbf{k}_\perp^2 \gamma^2].$$

Here \mathbf{k}_\perp denotes the deviation in the transverse direction from $\mathbf{0}$ and γ is proportional to the lattice spacing in the transverse directions a_\perp . We obtain

$$2T_\perp^2(\mathbf{0}) \gamma^2 \mathbf{k}_\perp^2 + \frac{b}{2} (q - q_0)^2 = T_\perp(\mathbf{0})^2 - (t_\perp^{\min})^2, \quad (47)$$

where

$$b = \frac{v_c^2}{Z_0^2} \frac{(x_0 + 1)(4\alpha x_0 - 3\alpha + 1)}{x_0(x_0 - 1)}.$$

We also can estimate the anisotropy of the Fermi surface from Eq. (47). The anisotropy of the masses is given by

$$\frac{m_\perp}{m_\parallel} = \frac{v_c^2}{4\gamma^2 m^2} \frac{(x_0 + 1)(4\alpha x_0 - 3\alpha + 1)}{x_0^3(1 + \alpha x_0)}, \quad (48)$$

where we have further approximated $T_\perp(\mathbf{0}) \approx t_\perp^{\min}$. Using that $v_c \approx 2ta_\parallel$, where a_\parallel is the lattice spacing along the chains, we find that

$$\frac{m_\perp}{m_\parallel} \approx \mathcal{A} \frac{a_\parallel^2}{\gamma^2 m^2} t^2, \quad (49)$$

where \mathcal{A} varies between 1.06 for $v_s \rightarrow v_c$ and 0.38 for $v_s \rightarrow 0$. Thus the magnitude of the mass ratio is determined by the competition of two factors one of which is large (t/m) and the other is small (a_\parallel/γ). As a result, the Fermi surface may not be very anisotropic.

An obvious question is whether or not the RPA can be trusted to describe correctly the formation of a Fermi surface. One problem of the RPA is that it automatically reproduces a purely one-dimensional result at the particular wave numbers \mathbf{p} where the transverse hopping vanishes $T_\perp(\mathbf{p}) = 0$. On a 2D square lattice with nearest-neighbor hopping this would be at the points $p_y = \pm \pi/2$. In the case of coupled Luttinger liquids the improved treatment of Ref. 11 indicates that in the vicinity of these points RPA is unreliable. In the case of coupled Mott insulators, the electron and hole pockets we find for sufficiently large t_\perp are located at positions far away from the points where $T_\perp(\mathbf{k})$ vanishes.

Recently a dynamical mean-field theory approach has been developed, which replaces the quasi-1D system by a single effective chain, from which electrons can hop to a self-consistent bath.^{30,31} The resulting model has to be analyzed by numerical methods and for coupled Hubbard chains it is found that for sufficiently large transverse hopping amplitudes an open Fermi surface (close to the one of the noninteracting model) is formed. This is in contrast to the electron and hole pockets we find in the RPA.

VI. TRANSVERSE CONDUCTIVITY AND DENSITY OF STATES

Using the results for uncoupled chains as well as the RPA expression for the Green's function of weakly coupled chains we can determine various other physical quantities.

A. The transverse conductivity

Let us consider a situation where the transverse hopping is only between nearest-neighbor chains. The transverse current operator is then given by

$$j_{\perp}(x,l) = iet_{\perp}[R_{\sigma}^{(l)}(x)R_{\sigma}^{(l+1)\dagger}(x) - \text{H.c.} + R \rightarrow L], \quad (50)$$

where l is a chain index and x denotes the position along the chain direction. Using this expression we can analytically determine the leading contribution in t_{\perp} to the transverse conductivity by using the result for the Green's function of uncoupled chains. We find

$$\sigma_{\perp}(\omega) = \frac{2Z_0^2 e^2 t_{\perp}^2}{\pi(v_c - v_s)} \frac{1}{\omega} \arctan \frac{4m\delta\sqrt{\omega^2 - 4m^2}}{\omega^2 + \delta(\omega^2 - 8m^2)}, \quad (51)$$

where $\delta = (v_c - v_s)/(v_c + v_s)$.

In the limit $v_s \rightarrow v_c = v$ this simplifies to

$$\sigma_{\perp}(\omega) = \frac{2Z_0^2 e^2 t_{\perp}^2}{\pi v} \frac{1}{\omega} (2m/\omega)^2 \sqrt{(\omega/2m)^2 - 1}. \quad (52)$$

We see that the transverse conductivity vanishes at the threshold $\omega = 2m$ and increases above it in a characteristic square-root fashion. This is reminiscent of the behavior found for the longitudinal conductivity in Ref. 23.

B. Density of states

Within the RPA we can determine the density of states (DOS) by integrating the RPA spectral function over all momenta. This needs to be done numerically. For simplicity we only consider the case $v_c = v_s = v$. For a 2D system³² with $T_{\perp}(k_y) = t_{\perp} \cos(k_y)$ we obtain the results shown in Fig. 9. As t_{\perp} is increased, the Mott gap in the DOS is filled in and eventually a peak forms around zero energy.

The analogous analysis for a quasi-3D system with $T_{\perp}(k_y, k_z) = t_{\perp} [\cos(k_y) + \cos(k_z)]$ yields a qualitatively different result. As t_{\perp} is increased the Mott gap is again filled in, but now the DOS around $\omega = 0$ remains basically flat and no peak develops in the regime where RPA applies, i.e., $t_{\perp}/m = O(1)$. In order to understand this result it is instructive to consider the case

$$T_{\perp}(\mathbf{k}) = t_{\perp} \sum_{j=1}^D \cos k_j, \quad D \gg 1. \quad (53)$$

In this limit $T_{\perp}(\mathbf{k})$ can be considered to be a random variable with probability distribution

$$P(t) = \frac{1}{\sqrt{\pi D t_{\perp}^2}} \exp\left(-\frac{t^2}{D t_{\perp}^2}\right). \quad (54)$$

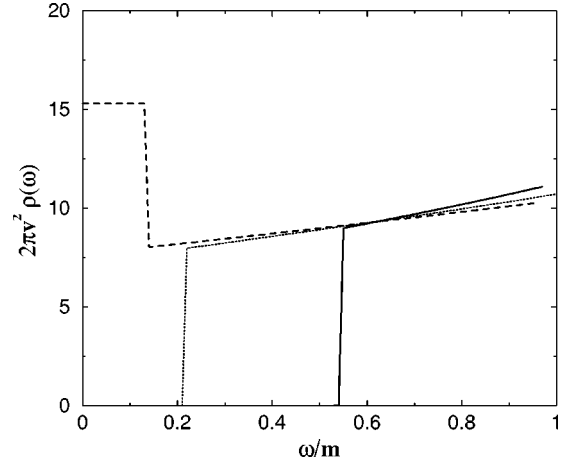


FIG. 9. Density of states for a 2D square lattice for frequencies smaller than the Mott gap. The curves are for $t_{\perp}=2$ (solid), $t_{\perp}=3$ (dotted), and $t_{\perp}=4$ (dashed).

As we are interested in the formation of a Fermi surface we have to consider $T_{\perp}(\mathbf{k}) = O(m)$, which implies that $t_{\perp}D/m = O(1)$. This leads to the restriction that for large D

$$t_{\perp} \propto \frac{m}{D}, \quad (55)$$

so that the probability distribution (54) becomes extremely narrow and only regions in k space with $T_{\perp}(\mathbf{k}) \approx 0$ contribute to the DOS. However, in these regions there are no states at $\omega \approx 0$ and there will, therefore, be no peak in the DOS at low energies.

VII. BECHGAARD SALTS AS A POSSIBLE APPLICATION

Our theory may be relevant to the Bechgaard salts and in particular to $(\text{TMTTF})_2\text{PF}_6$ and $(\text{TMTSF})_2\text{PF}_6$ (see Refs. 33,34 for a review). However, for our theory to be relevant, certain conditions must be met and this requires a discussion. The materials in question are quasi-one-dimensional and have a three-fourth-filled band. The ratio of the hopping integrals in the three principal crystallographic directions is $t_a:t_b:t_c \approx 1:0.1:0.005$. Therefore, at sufficiently high temperatures one may neglect the hopping in the c direction. Then one is left with a two-dimensional system, where each chain has only two nearest neighbors ($\mathcal{N}=2$). The interchain hopping is not long ranged, which puts into question the reliability of RPA. We urge the reader to keep this caveat in mind during the following discussion.

The principal problem one encounters in dealing with the Bechgaard salts is the problem identifying the correct low-energy effective theory. Let us neglect the interchain hopping for the time being and consider uncoupled 1D chains. In the Bechgaard salts there are two separate mechanisms that have the potential to open a spectral gap. First there are ‘‘double’’ Umklapp processes due to the commensurate band filling $3/4$.^{35,36} These processes involve the scattering of four electrons at k_F and four holes at $-k_F$ and are generated in the low-energy effective theory by integrating out high-energy modes. These processes will generate a gap only for strong

interactions ($K_c < 0.25$). Second, there is a small dimerization, which halves the Brillouin zone and gives rise to “single” Umklapp processes.^{37,38} These open a gap already for weak interactions $K_c < 1$ but their coupling constant is proportional to the dimerization and thus small. At low energies the system is thus described by two independent Gaussian models—one for the charge and the other for the spin sector. The charge-sector Gaussian model is perturbed by two operators: the $4k_F$ harmonics (with k_F being equal to $3\pi/2a$) of the dimerization

$$\hat{D} = \delta t \sum_n (-1)^n c_{n+1,\sigma}^+ c_{n,\sigma}, \quad (56)$$

where δt is a staggered component of the hopping integral, and the $8k_F$ component of the electron-density operator (double-Umklapp processes). Since these operators have different symmetry under parity transformation (one is defined on links and the other on sites), in the continuous limit they are given by sin and cos, respectively, such that the related Hamiltonian density is

$$V = g_1 \sin(\sqrt{8\pi K_c} \Phi_c) + g_2 \cos(2\sqrt{8\pi K_c} \Phi_c). \quad (57)$$

The behavior of the system and applicability of our theory depend crucially on the value of K_c . We can consider the following possibilities.

(i) The interactions are weak and $K_c \approx 1$.^{37,39} A moderate interaction strength is suggested by the renormalization of the uniform magnetic susceptibility with respect to the value extracted from band-structure calculation $\chi_s/\chi_0 \approx 2-3$.³⁴ In this case, the g_2 term in Eq. (57) is irrelevant and the first term (due to dimerization) gives a sine-Gordon model (SGM) that is equivalent to the charge sector of the Thirring model we have discussed. All our calculations are valid in this case.

If we adopt this scenario we have problems with angle-resolved photoemission (ARPES) data that do not show any traces of quasiparticles.^{40,41} We will return to the question about ARPES data later.

(ii) There is a school of thought that advocates the small value $K_c \approx 0.22$ when both operators are relevant.^{35,42} According to this school, the dimerization coupling is small and the g_2 term dominates. This would agree qualitatively with the ARPES data.

If this point of view is correct, the calculations presented in this paper are not applicable because, as it follows from Ref. 15, for such values of K_c the minimal form factor corresponds to the emission of not one, but two solitons. We have discussed this scenario elsewhere.⁴³ Here we cite just one conclusion of Ref. 43: if K_c is small and the dimerization term is negligible, the value of the gap measured by ARPES should be equal to the optical gap observed in the frequency dependence of the on-chain conductivity, or twice the value of the activation gap in the temperature dependence of the dc conductivity

$$\Delta_{\text{ARPES}} = 2E_{\text{act}} = \Delta_{\text{opt}} = 2m. \quad (58)$$

Indeed, in $(\text{TMTTF})_2\text{PF}_6$ ARPES measures a gap $\Delta \approx 100$ meV and thermal-conductivity measurements give the activation gap $E_{\text{act}} = 44$ meV,⁴⁴ which is roughly one-half.

(iii) The third possible scenario is that K_c is small, but the dimerization is not negligible. In this case one has to deal with a two-frequency sine-Gordon model.⁴⁵ To get a qualitative idea of what happens in this situation it is essential to estimate the bare values of the coupling constants $g_{1,2}$. We know how to do this only at weak coupling, where perturbation theory for a quarter filled, extended Hubbard model with (next) nearest-neighbor density-density coupling V_1 (V_2), gives the following estimate³⁶

$$g_2 \propto \frac{a_0}{t^2} [(U - 2V_2)^2 (U - 4V_1 + V_2) + 4V_2^2 (U - 2V_1 + 2V_2)]. \quad (59)$$

Note that we need to consider an extended Hubbard model because without $V_{1,2}$ it is not possible to obtain a sufficiently small value of K_c for the g_2 term to become relevant.⁴⁶

If both terms are relevant and the sign of g_2 is *positive* then the g_1 term leads to the confinement of the solitons in the g_2 -sine-Gordon model. This is a difficult case to handle as the two-frequency SGM is not integrable.

If, on the other hand, g_2 is *negative*, as is possible in the perturbative result (59) for sufficiently strong V_1 , then the g_1 term does not lead to a qualitative change of the physics of the $g_1 = 0$ model. In this case the effects of dimerization will not be essential.

Let us assume for the time being that $K_c \approx 1$ and see how our theory would compare with experiment. $(\text{TMTTF})_2\text{PF}_6$ is a Mott insulator; the Fermi energy is estimated as 115 meV, the hopping integral in the b direction is of the order of 14 meV, the optical gap $\Delta_{\text{opt}} = 2m$ is approximately 900 K. Here the transverse tunneling is not large enough to overcome the Mott gap. In trying to get a detailed comparison with our calculations one has to take into account that the ratio $m/\epsilon_F \approx 1/3$ is not very small here, which reduces the chances of obtaining a quantitative agreement with any field-theoretical approach.

$(\text{TMTSF})_2\text{PF}_6$ is metallic; the Fermi energy is estimated as 220 meV, the hopping integral in the b direction is roughly 20 meV, the optical gap $\Delta_{\text{opt}} = 2m$ is of the order of 250 K. This gives $T_{\perp}(0)/m \approx 4$ so that the criterion for having a small Fermi surface $Z_0 T_{\perp}(0)/m > 3.3$ is satisfied here. Optical measurements for this material show a metallic Drude peak with a tiny amount of spectral weight (3%), separated by a gap from a very strong continuum. The metallic character of these compounds is due to the transverse hopping.^{44,47} For frequencies not too close to the gap the observed form of the optical conductivity in the direction along the chains is well described by the sine-Gordon model.²³ This fact, together with the observed smallness of the Drude weight, indicates that $(\text{TMTSF})_2\text{PF}_6$ may be a candidate for application of the present theory.

An additional argument in favor of small pockets of Fermi liquid is that not all physical properties of $(\text{TMTSF})_2\text{PF}_6$ demonstrate the same degree of anisotropy. For example, the

measured anisotropy of the plasma frequency for the Drude peaks is only of a factor of 2.⁴⁸ On the other hand, for the ratio of hopping integrals predicted by the band theory one should expect it to be of order of $(m_{\perp}/m_{\parallel})^{1/2} \approx 10$. This fact, in combination with the smallness of the Drude weight, indicates that the Fermi surface is small and not very anisotropic. On the other hand, many of the properties of these materials (especially the magnetic ones) are typically one dimensional (see Ref. 34 for a review). Thus the overall picture is in reasonable agreement with the scenario we present.

The analysis of the Drude peak given in Ref. 42 indicates that the best fit can be obtained if one assumes frequency-dependent effective mass and the scattering rates in the Drude formula

$$\sigma(\omega) = \frac{\omega_p^2}{4\pi} \frac{1}{\Gamma_1(\omega) - i\omega \left[\frac{m^*(\omega)}{m_{\text{band}}} \right]},$$

$$\frac{m^*(\omega)}{m_{\text{band}}} = 1 + \frac{\lambda_0}{1 + \alpha^2 \omega^2},$$

$$\Gamma_1(\omega) = \Gamma_0 + \frac{\lambda_0 \alpha \omega^2}{1 + \alpha^2 \omega^2}. \quad (60)$$

Here Γ_0 and λ_0 are the zero-frequency scattering rate and mass-enhancement factor, respectively.⁴² This fit is rather suggestive because the frequency dependence is quadratic, such as in Fermi-liquid theory. This feature supports the point of view that the Drude peak comes from small pockets of Fermi liquid.

There are other quasi-one-dimensional systems for which ARPES measurements have been performed: the blue bronze $\text{K}_{0.3}\text{MoO}_3$, which is metallic,⁴⁹ and the Mott insulator Sr_2CuO_3 . The latter material, however, is not a good testing ground for our theory since the ratio of the Mott-Hubbard gap to the bandwidth is too large. The largeness of the gap precludes a detailed comparison with the results obtained in this paper. On the qualitative side the measurements demonstrate the appearance of two distinct dispersing maxima in the spectral function,⁵⁰ which is interpreted as a sign of spin-charge separation.

ARPES is not the only way to ascertain the existence of quasiparticles. de Haas-van Alphen and Schubnikov-de Haas effects are perfect tools when one deals with closed Fermi surfaces. Obviously, the measurements should be made above the ordering temperature that may impose serious difficulties.

ACKNOWLEDGMENTS

This work was started at the Isaac Newton Institute for Mathematical Sciences in Cambridge during the program on Strongly Correlated Electrons in 2000. We are grateful to the Institute for hospitality. Our warmest thanks are to Sergei Lukyanov for his help and interest in the work. We acknowledge illuminating conversations with A. Chubukov, N. D'Ambrumenil, A. Finkelstein, F. Gebhard, A. Georges, T.

Giamarchi, P. Wiegmann, and V. Yakovenko. We also thank S. Kivelson and D. Orgad for useful correspondence. This work was supported by the EPSRC under Grants Nos. AF/100201 and GR/N19359 (FHLE) and by the DOE under Contract number DE-AC02-98 CH 10886.

APPENDIX A: ELEMENTS OF RPA

In this appendix we discuss some relevant aspects of the RPA in the interchain coupling. This is most easily done in position space. We denote the right-moving and left-moving fermion operators by black and white dots. 1D correlation functions are denoted by encircling a number of dots, the corresponding fermion operators are then all located on the same chain. In Fig. 10 we show the corresponding diagrams for the 1D two-point functions of right movers and left movers as well as the diagram for the $2n$ -point function of right movers. Finally, we denote the interchain hopping matrix element $t_{ij}(x-y)$ between sites x/a_0 on chain i and site y/a_0 on chain $j \neq i$ by a dashed line. We note that the hopping is local in time.

The first few diagrams in the expansion (in the interchain hopping) of the two-point function of right-moving electrons for initial and final point located on the same chain is shown in Fig. 11. The contribution of a given diagram is obtained by summing over the positions of all ‘‘internal’’ circles, that is, connected by a hopping line.

The RPA expression for the Fourier transform of the single-particle Green's function is obtained by summing all diagrams that can be split into two parts by cutting any one hopping line, i.e., all diagrams of the type shown in Fig. 12.

All diagrams neglected in RPA contain loops. This enables us to embed RPA into a systematic perturbative expansion in a small parameter κ_0 as follows. Let us consider an interchain hopping $T_{\perp}(\mathbf{k})$ (for simplicity we take it independent of the wave number q along the chain direction) of the form shown in Fig. 13 i.e., particle-hole symmetric but long ranged such that its Fourier transform is strongly peaked around the origin and the point $(0, \pi, \pi)$. This means that in position space the hopping is *long ranged*, i.e., the hopping amplitudes are of the same order within a range proportional to κ_0^{-1} .

Every loop gives a contribution

$$\frac{1}{V} \sum_{\mathbf{k}} [T_{\perp}(\mathbf{k})]^2 \propto \kappa_0^2 \quad (A1)$$

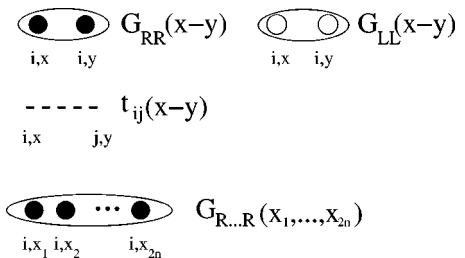


FIG. 10. Elements of the diagram technique in position space. Only one kind of many-particle ‘‘vertex’’ is shown.

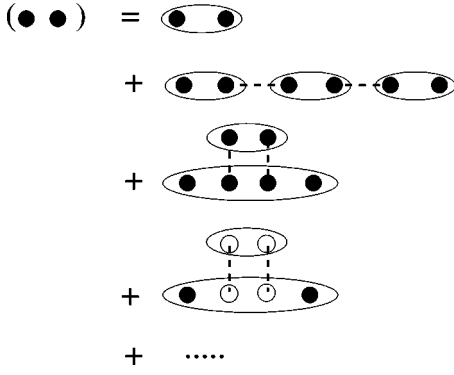


FIG. 11. Diagrams for initial and final points on the same chain up to second order in the interchain hopping.

and is thus suppressed. In this way one obtains a formal expansion in powers of κ_0^2 , the leading (κ_0^0) order of which is given by the RPA.

APPENDIX B: FORM-FACTOR APPROACH IN INTEGRABLE QUANTUM-FIELD THEORIES

The spectrum of low-lying excitations of the half-filled Hubbard model consists of scattering states of gapped, spinless charge $\pm e$ excitations called *holons* and *antiholons* and gapless, charge-neutral excitations carrying spin $\pm \frac{1}{2}$, the so-called *spinons*.⁵¹ We introduce labels h, \bar{h}, s, \bar{s} to distinguish between these four types of elementary excitations. Their dispersions and exact scattering matrices are known on the lattice⁵¹ as well as in the field-theory limit.⁵² As usual for particles with relativistic dispersion it is useful to introduce rapidity variables $\theta_{c,s}$ to parametrize energy and momentum

$$E_\alpha(\theta_c) = m \cosh \theta_c, \quad P_\alpha(\theta_c) = m \sinh \theta_c, \quad \alpha = h, \bar{h},$$

$$E_\gamma(\theta_s) = \frac{m}{2} e^{\pm \theta_s}, \quad P_\gamma(\theta_s) = \pm \frac{m}{2} e^{\pm \theta_s}, \quad \gamma = s, \bar{s}. \quad (\text{B1})$$

Here we have set spin and charge velocities to 1. Let us now turn to the construction of a basis of scattering states of holons, antiholons, and spinons. A convenient formalism to this end is obtained in terms of the Zamolodchikov-Faddeev (ZF) algebra. The ZF algebra can be considered to be the extension of the algebra of creation and annihilation operators for free fermion or bosons to the case of interacting particles with factorizable scattering. The ZF algebra is based on the knowledge of the exact spectrum and scattering matrix. For the SGM, the ZF operators (and their Hermitian conjugates) satisfy the following algebra:

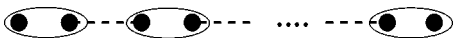


FIG. 12. Diagrams entering the RPA expression for the single-particle Green's function. The sum is over all diagrams of the type shown.

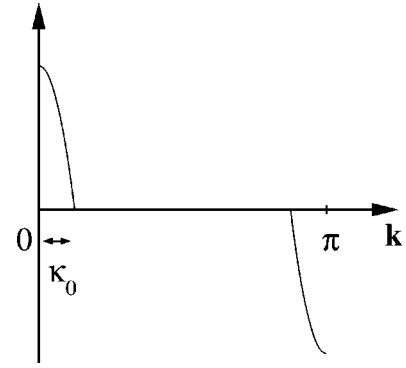


FIG. 13. Schematic dependence of $T_\perp(\mathbf{k})$ on the transverse momenta q_\perp .

$$\begin{aligned} Z^{\epsilon_1}(\theta_1) Z^{\epsilon_2}(\theta_2) &= S_{\epsilon'_1, \epsilon'_2}^{\epsilon_1, \epsilon_2}(\theta_1 - \theta_2) Z^{\epsilon'_2}(\theta_2) Z^{\epsilon'_1}(\theta_1), \\ Z_{\epsilon_1}^\dagger(\theta_1) Z_{\epsilon_2}^\dagger(\theta_2) &= Z_{\epsilon_2'}^\dagger(\theta_2) Z_{\epsilon_1'}^\dagger(\theta_1) S_{\epsilon_1, \epsilon_2}^{\epsilon_1', \epsilon_2'}(\theta_1 - \theta_2), \\ Z^{\epsilon_1}(\theta_1) Z_{\epsilon_2}^\dagger(\theta_2) &= Z_{\epsilon_2'}^\dagger(\theta_2) S_{\epsilon_2, \epsilon_1'}^{\epsilon_2, \epsilon_1}(\theta_2 - \theta_1) Z^{\epsilon_1'}(\theta_1) \\ &\quad + (2\pi) \delta_{\epsilon_2}^{\epsilon_1} \delta(\theta_1 - \theta_2). \end{aligned} \quad (\text{B2})$$

Here $S_{\epsilon'_1, \epsilon'_2}^{\epsilon_1, \epsilon_2}(\theta)$ are the (factorizable) two-particle scattering matrices and $\varepsilon_j = s, \bar{s}, h, \bar{h}$.

Using the ZF generators a Fock space of states can be constructed as follows. The vacuum is defined by

$$Z_{\varepsilon_i}(\theta) |0\rangle = 0. \quad (\text{B3})$$

Multiparticle states are then obtained by acting with strings of creation operators $Z_\epsilon^\dagger(\theta)$ on the vacuum

$$|\theta_n \dots \theta_1\rangle_{\varepsilon_n \dots \varepsilon_1} = Z_{\varepsilon_n}^\dagger(\theta_n) \dots Z_{\varepsilon_1}^\dagger(\theta_1) |0\rangle. \quad (\text{B4})$$

In terms of this basis the resolution of the identity is given by

$$\sum_{n=0}^{\infty} \sum_{\varepsilon_i} \int_{-\infty}^{\infty} \frac{d\theta_1 \dots d\theta_n}{(2\pi)^n n!} |\theta_n \dots \theta_1\rangle_{\varepsilon_n \dots \varepsilon_1} \langle \varepsilon_1 \dots \varepsilon_n | \theta_1 \dots \theta_n|. \quad (\text{B5})$$

Inserting Eq. (B5) between operators in a two-point function we obtain the following spectral representation

$$\begin{aligned} \langle \mathcal{O}(x, t) \mathcal{O}^\dagger(0, 0) \rangle &= \sum_{n=0}^{\infty} \sum_{\varepsilon_i} \int \frac{d\theta_1 \dots d\theta_n}{(2\pi)^n n!} \\ &\quad \times \exp \left[i \sum_{j=1}^n P_{\varepsilon_j}(\theta_j) x - E_{\varepsilon_j}(\theta_j) t \right] \\ &\quad \times |\langle 0 | \mathcal{O}(0, 0) | \theta_n \dots \theta_1 \rangle_{\varepsilon_n \dots \varepsilon_1}|^2, \end{aligned} \quad (\text{B6})$$

where

$$f^\mathcal{O}(\theta_1 \dots \theta_n)_{\varepsilon_1 \dots \varepsilon_n} \equiv \langle 0 | \mathcal{O}(0, 0) | \theta_n \dots \theta_1 \rangle_{\varepsilon_n \dots \varepsilon_1} \quad (\text{B7})$$

are the form factors.

- ¹N.F. Mott, *Metal-Insulator Transitions*, 2nd ed. (Taylor and Francis, London, 1990); F. Gebhard, *The Mott Metal-Insulator Transition* (Springer, Berlin, 1997).
- ²N.F. Mott, Proc. R. Soc. London, Ser. A **62**, 416 (1949); Can. J. Phys. **34**, 1356 (1964); Philos. Mag. **6**, 287 (1961).
- ³J. Hubbard, Proc. R. Soc. London, Ser. A **284**, 401 (1964).
- ⁴L.B. Ioffe and A.I. Larkin, Phys. Rev. B **39**, 8988 (1989).
- ⁵G. Kotliar and J. Liu, Phys. Rev. Lett. **61**, 1784 (1988); M. Grilli and G. Kotliar, *ibid.* **64**, 1170 (1990).
- ⁶A. Georges, G. Kotliar, W. Krauth, and M.J. Rozenberg, Rev. Mod. Phys. **68**, 13 (1996).
- ⁷W. Metzner and D. Vollhardt, Phys. Rev. Lett. **62**, 324 (1989); D. Vollhardt, Int. J. Mod. Phys. B **3**, 2189 (1989).
- ⁸R.M. Noack and F. Gebhard, Phys. Rev. Lett. **82**, 1915 (1999).
- ⁹X.G. Wen, Phys. Rev. B **42**, 6623 (1990).
- ¹⁰D. Boies, C. Bourbonnais, and A.-M.S. Tremblay, Phys. Rev. Lett. **74**, 968 (1995).
- ¹¹E. Arrigoni, Phys. Rev. B **61**, 7909 (2000).
- ¹²E. Jeckelmann, F. Gebhard, and F.H.L. Essler, Phys. Rev. Lett. **85**, 3910 (2000).
- ¹³A.O. Gogolin, A.A. Nersisyan, and A.M. Tsvelik, *Bosonization and Strongly Correlated Systems* (Cambridge University Press, Cambridge, 1999).
- ¹⁴F. A. Smirnov, *Form Factors in Completely Integrable Models of Quantum Field Theory* (World Scientific, Singapore, 1992); M. Karowski and P. Weisz, Nucl. Phys. B **139**, 455 (1978); H. Babujian, A. Fring, M. Karowski, and A. Zapletal, *ibid.* **538**, 535 (1999); A. Fring, G. Mussardo, and P. Simonetti, *ibid.* **393**, 413 (1993).
- ¹⁵S. Lukyanov and A.B. Zamolodchikov, Nucl. Phys. B **607**, 437 (2001).
- ¹⁶G. Delfino and G. Mussardo, Nucl. Phys. B **455**, 724 (1995).
- ¹⁷P. B. Wiegmann, in *Soviet Science Review Series A*, edited by I. M. Khalatnikov (Harwood, Cambridge, 1980), Vol. 2, p. 41.
- ¹⁸J. Voit, Eur. Phys. J. B **5**, 505 (1998).
- ¹⁹O.A. Starykh, D.L. Maslov, W. Heusler, L.I. Glazman, in *Low-Dimensional Systems*, edited by T. Brandes, Lecture Notes in Physics (Springer, Berlin, 2000)
- ²⁰D. Orgad, Philos. Mag. B **81**, 377 (2001).
- ²¹A. Parola and S. Sorella, Phys. Rev. B **45**, 13 156 (1992), **57**, 6444 (1998).
- ²²M.B. Halpern, Phys. Rev. D **12**, 1684 (1976); R. Köberle, V. Kurak, and J.A. Swieca, *ibid.* **20**, 897 (1979).
- ²³D. Controzzi, F.H.L. Essler, and A.M. Tsvelik, Phys. Rev. Lett. **86**, 680 (2001).
- ²⁴B.A. Bernevig, D. Giuliano, and R.B. Laughlin, cond-mat/0105523 (unpublished).
- ²⁵V. Meden and K. Schönhammer, Phys. Rev. B **46**, 15 753 (1992).
- ²⁶R.N. Bannister and N. d'Ambrumenil, Phys. Rev. B **61**, 4651 (2000); R. N. Bannister, Ph.D. thesis, University of Warwick, 1998.
- ²⁷S. Nishimoto, E. Jeckelmann, F. Gebhard, and R. Noack, cond-mat/0110420.
- ²⁸P.W. Anderson, Phys. Rev. Lett. **67**, 3844 (1991).
- ²⁹I. E. Dzyaloshinskii (unpublished).
- ³⁰A. Georges, T. Giamarchi, and N. Sandler, Phys. Rev. B **61**, 16 393 (2000).
- ³¹S. Biermann, T. Giamarchi, A. Georges, and A. Lichtenstein, Phys. Rev. Lett. **87**, 276405 (2001).
- ³²Here we consider transverse hopping between nearest neighbor chains, so that RPA is not a controlled approximation.
- ³³T. Ishiguro and K. Yamji, *Organic Superconductors* (Springer-Verlag, Berlin, 1990).
- ³⁴C. Bourbonnais and D. Jerome, in *Advances in Synthetic Metals, Twenty Years of Progress in Science and Technology*, edited by P. Bernier, S. Lefrant, and G. Bidan (Elsevier, New York, 1999), pp. 206-301 and references therein; See also cond-mat/9903101 (unpublished).
- ³⁵T. Giamarchi, Physica B **230-232**, 975 (1997).
- ³⁶H. Yoshioka, M. Tsuchizu, and Y. Suzumura, J. Phys. Soc. Jpn. **70**, 762 (2001).
- ³⁷V.J. Emery, R. Bruinsma, and S. Barisic, Phys. Rev. Lett. **48**, 1039 (1982).
- ³⁸K. Penc and F. Mila, Phys. Rev. B **50**, 11 429 (1994).
- ³⁹S. Brazovskii and V. Yakovenko, Sov. Phys. JETP **62**, 1340 (1985).
- ⁴⁰F. Zwick, S. Brown, G. Margaritondo, C. Merlic, M. Onellion, J. Voit, and M. Grioni, Phys. Rev. Lett. **79**, 3982 (1997).
- ⁴¹T. Valla and P. Johnson (unpublished).
- ⁴²A. Schwartz, M. Dressel, G. Grüner, V. Vescoli, L. Degiorgi, and T. Giamarchi, Phys. Rev. B **58**, 1261 (1998).
- ⁴³F.H.L. Essler and A.M. Tsvelik, Phys. Rev. Lett. **88**, 096403 (2002).
- ⁴⁴V. Vescoli, L. Degiorgi, W. Henderson, G. Grüner, K.P. Starkey, and L.K. Montgomery, Science **281**, 1181 (1998).
- ⁴⁵G. Delfino and G. Mussardo, Nucl. Phys. B **516**, 675 (1998); M. Fabrizio, A.O. Gogolin, and A.A. Nersisyan, *ibid.* **580**, 647 (2000).
- ⁴⁶H. Frahm and V.E. Korepin, Phys. Rev. B **43**, 5653 (1991).
- ⁴⁷T. Giamarchi, Physica B **230-232**, 975 (1997).
- ⁴⁸W. Henderson, V. Vescoli, P. Tran, L. Degiorgi, and G. Grüner, Eur. Phys. J. B **11**, 365 (1999).
- ⁴⁹G.H. Gweon, J.W. Allen, R. Claessen, J.A. Clack, D.M. Poirier, P.J. Benning, C.G. Olson, W.P. Ellis, X.Y. Zhang, L.F. Schneemeyer, J. Marcus, and G. Schlenker, J. Phys.: Condens. Matter **8**, 9923 (1996).
- ⁵⁰C. Kim, Z.X. Shen, N. Montoyama, H. Eisaki, S. Uchida, T. Tohyama, and S. Maekawa, Phys. Rev. B **56**, 15 589 (1997).
- ⁵¹F.H.L. Essler and V.E. Korepin, Phys. Rev. Lett. **72**, 908 (1994); Nucl. Phys. B **426**, 505 (1994).
- ⁵²E. Melzer, Nucl. Phys. B **443**, 553 (1995).